



U.S. Department of the Interior

U.S. Geological Survey

Western Ecological Research Center

## 2025 Project Summary

### Sea-level rise vulnerability of tidal wetlands in south San Francisco Bay

Prepared for U.S. Fish & Wildlife Service, South Bay Salt Pond Restoration Project, and California  
Wildlife Foundation

**Prepared by:** Kevin Buffington<sup>1</sup>, Karen Thorne<sup>1</sup>, Tom Lorenson<sup>2</sup>, Peter Swarzenski<sup>2</sup>

<sup>1</sup>US Geological Survey, Western Ecological Research Center, Davis, CA, [kbuffington@usgs.gov](mailto:kbuffington@usgs.gov),  
[kthorne@usgs.gov](mailto:kthorne@usgs.gov), 916-502-2996

<sup>2</sup>Retired, US Geological Survey, Pacific Coastal and Marine Center, Santa Cruz, CA

## Abstract

Projected accelerations in the rate of sea-level rise (SLR) later this century have the potential to structurally reshape the coastal environment. We sought to assess the vulnerability of tidal marsh habitats to be lost or altered due to SLR across Don Edwards San Francisco Bay National Wildlife Refuge in south San Francisco Bay using extensive field datasets including baseline surveys of marsh surface elevation and vegetation as well as soil characteristics and accretion rates derived from soil cores. Across eight marsh parcels we collected three 1 m deep soil cores in low, mid, and high marsh zones, and processed them for bulk density (mean =  $0.39 \pm 0.05 \text{ g cm}^{-3}$ ) and organic matter percent (mean =  $12.7 \pm 3.8\%$ ). A subset of cores was dated using gamma spectroscopy methods; four cores had usable data for the calculation of accretion rates (Mowry:  $0.29 \text{ cm yr}^{-1}$ , Triangle:  $0.38 \text{ cm yr}^{-1}$ , Guadalupe Slough:  $0.91 \text{ cm yr}^{-1}$ , and Coyote Creek Lagoon:  $0.67 \text{ cm yr}^{-1}$ ). We had a low success rate using radioisotopes to date soil cores, likely due to extensive sediment resuspension that occurs across south San Francisco Bay. Data from these four sites were then used to calibrate WARMER3, a biogeomorphic model of wetland soils and projected future elevation, plant species composition, and carbon accumulation under four SLR scenarios and three sediment availability scenarios. The model showed that all marshes persisted under the low SLR scenario, which simulated the continuation of historic SLR without rapid acceleration. Under intermediate SLR ( $\sim +1 \text{ m}$  by 2100), all four marshes persisted, however Mowry and Triangle were projected to convert from a pickleweed-dominant high marsh to *Spartina*-dominant low marsh. With intermediate high SLR scenario ( $\sim +1.5 \text{ m}$  by 2100) Mowry and Triangle were projected to convert to an unvegetated state and Guadalupe Slough to *Spartina*-dominant, while with high

(~+2 m by 2100) SLR, Mowry, Triangle, and Coyote Creek Lagoon were projected to become unvegetated by the end of the century; only Guadalupe Slough was projected to persist as a vegetated marsh under the highest SLR scenario. Changing sediment availability altered marsh vulnerability at Guadalupe Slough and Coyote Creek Lagoon but had minor effects at the other two sites. This study highlights marsh resilience under low or modest SLR projections, primarily due to high sediment availability and accretion rates, but vulnerability under higher rates of SLR. It also demonstrates the challenges in using radioisotopes to measure accretion rates in a part of the estuary that is subject to extensive sediment resuspension. Long-term contemporary monitoring of accretion in south San Francisco Bay is critical to understand SLR vulnerability as the estuary conditions continue to change.

## **Introduction**

Acceleration in sea-level rise (SLR) projected this century has the potential to structurally reshape coastlines and put tidal ecosystems at risk (Wright and Thom 2023). Tidal saline marshes are at particular risk of conversion to an unvegetated state if the natural processes that contribute to increases in elevation are unable to keep pace with SLR (Kirwan and Megonigal 2013; Cahoon 2015). Dense marsh vegetation promotes the settling of suspended sediment on the surface (Stumpf 1983; Boorman et al. 1998), while belowground, root production and turnover increases soil volume and contribute to elevation gains (Gosselink et al 2984; Blum 1993). Regular flooding creates conditions that slow the rate of decomposition, resulting in the development of deep

layers of organic peat (Howarth and Hobbie 1982; Stagg et al. 2017). Numerical models that capture these processes and their inherent feedbacks are one tool available to resource managers to assess future marsh vulnerability and can aid the development of mitigation and restoration strategies.

Prior efforts to understand future vulnerability around San Francisco Bay have generally focused on marshes in central San Francisco Bay, San Pablo Bay, and Suisun Bay (WARMER, Swanson et al. 2014, 2015; MEM, Schile et al. 2014; WARMER2, Buffington et al. 2021; CWEM, Morris et al. 2022). In this project (Phase II) we assessed the vulnerability of marshes to SLR across south San Francisco Bay within the Don Edwards San Francisco Bay National Wildlife Refuge using the WARMER3 modeling framework (Buffington et al. 2024) and baseline elevation and vegetation datasets that were collected during Phase I (Thorne et al. 2019, Rankin et al. 2024).

## **Methods**

### *Study site*

Don Edwards San Francisco Bay National Wildlife Refuge (DENWR, refuge) is in south San Francisco Bay and was established in 1972 to support migratory waterbirds and protect critical marsh habitat for endangered wildlife species including the salt marsh harvest mouse (*Reithrodontomys raviventris*), California Ridgway's rail (*Rallus obsoletus obsoletus*), and Western snowy plover (*Anarhynchus nivosus nivosus*) (Don Edwards 2012). Roughly 3295 ha of tidal marsh is found within the refuge boundaries, existing within a patchwork mosaic of urban development, operational and retired salt production ponds, subsided ponds breached for natural tidal

restoration, and extensive mudflats (Don Edwards 2012). Levees or road surround nearly all the marshes in DENWR, which effectively eliminates upslope transgression as a potential response to SLR; if the DENWR marshes are to persist, they will need to accrete vertically at rates that offset SLR and not contract horizontally (Thorne et al. 2025).

### *Field data*

In August 2022 we collected soil cores with a 1 m gouge auger (n=24, Fig. 1) across eight marsh parcels in DENWR (Fig. 1). Cores were sliced in the field (2 cm intervals from 0-20 cm, 4 cm intervals > 20 cm; Mackenzie et al. 2016) and dried to constant mass for calculation of bulk density (core cross-section=27.776 cm<sup>2</sup>). The dried slices were homogenized using a mortar and pestle and a ~2 g subsample was placed in a 500°C muffle furnace for 4 hours to determine the organic fraction via loss-on-ignition.

To estimate accretion rates, 13 soil cores were sent to laboratories with gamma spectrometry and dated using <sup>210</sup>Pb and <sup>137</sup>Cs radioisotopes. <sup>210</sup>Pb is a naturally occurring radioisotope that precipitates from the atmosphere and attaches to fine soil particles. In undisturbed marsh soils, the radioactive decay of <sup>210</sup>Pb can be modeled with depth to estimate an accretion rate. <sup>137</sup>Cs in soils are a legacy of atmospheric nuclear bomb testing; peak <sup>137</sup>Cs first appeared in soils in 1955 and peaked in 1963/64 with the banning of atmospheric testing (Ritchie and McHenry 1990). However, of the 13 soil cores sent for radioisotope dating, just three had <sup>210</sup>Pb profiles that were suitable for calculating accretion, while one had a clear peak in <sup>137</sup>Cs. All other soil cores did not have detectable radioactivity needed for dating. These four soil cores,

sampled from four different marsh parcels (Mowry, Triangle, Guadalupe Slough and Coyote Creek Lagoon), were used as the basis for calibrating the WARMER3 model and projecting marsh resilience to future SLR. Given the difficulty detecting clear signals in radioactivity, the lab recommended against dating the remaining cores and to base the analysis on the four cores. Given the variation in accretion rates observed, we opted not to extrapolate our model results to other marshes.

We leveraged marsh elevation and vegetation surveys that were conducted in 2017 across 39 marsh parcels to inform the model (Rankin et al. 2024, Thorne et al. 2019). Shore-normal transects were established to sample across marsh elevation and plant density gradients; elevation was measured every 12.5 m with real-time kinematic GPS (Leica Geosystems, accuracy  $\pm 2$  cm) and vegetation was surveyed every 25 m within 0.25 m<sup>2</sup> quadrats. Species cover and

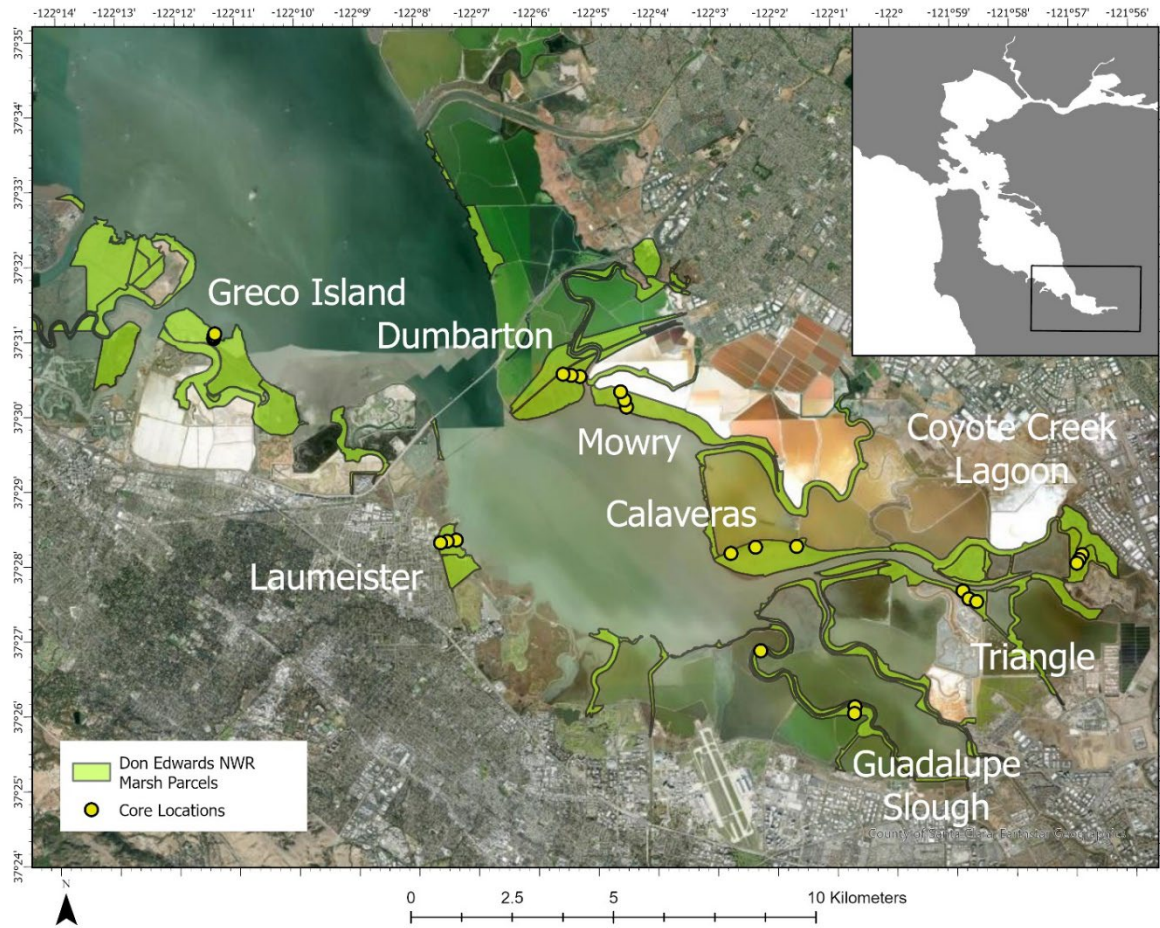


**Figure 1.** Soil coring locations across Don Edwards San Francisco Bay National Wildlife Refuge in south San Francisco Bay, CA. Basemap imagery is from County of Santa Clara Maxar.

height were recorded. These data were used to define the elevation niche needed for modeling of the dominant species *Salicornia pacifica*, *Spartina foliosa*, and *Schoenoplectus americanus* (Fig. 2).

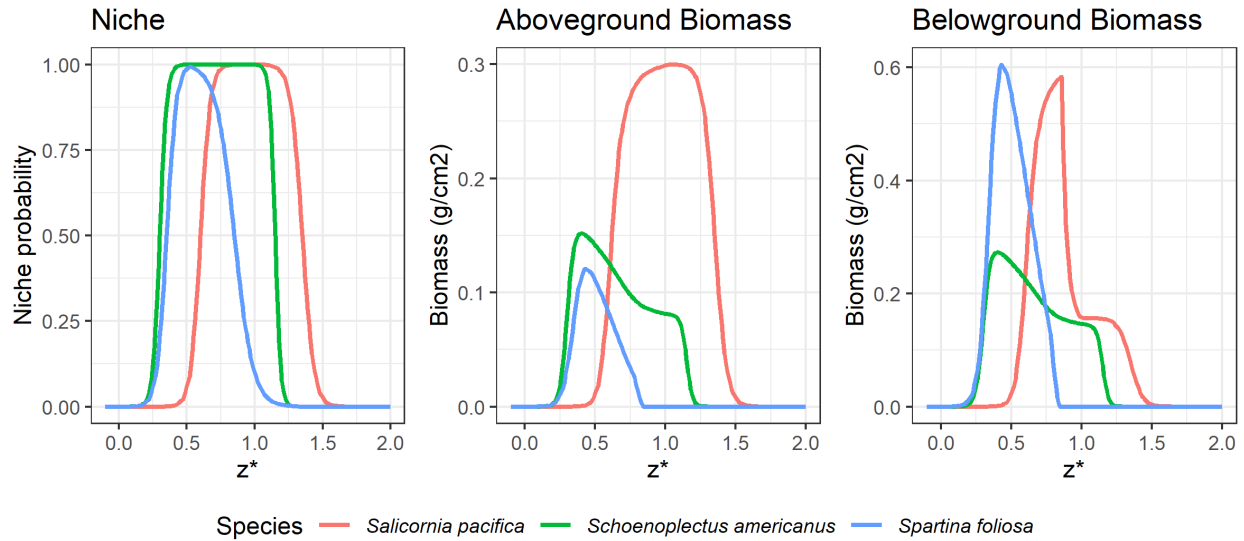


**Figure 2.** Species niche and maximum biomass functions across normalized elevation. Species niches were defined by field surveys across Don Edwards National Wildlife Refuge. Aboveground biomass was informed by marsh organ experiments. The root-to-shoot ratio was a function of flooding time in the case of *Salicornia pacifica* and *Spartina foliosa* (Janousek et al. 2016), while a root-to-shoot value of 1.8 was used for *Schoenoplectus americanus*.  $z^*$  is elevation relative to mean sea level divided by half the tidal range; zero is mean sea level and one is the upper tidal range.

### Model calibration

WARMER3 is a 1D soil cohort model for simulating tidal wetland responses to SLR (Buffington et al. 2024). It captures the dominant above and belowground processes responsible for vertical changes in wetland soils, including root growth and turnover, organic decomposition, soil consolidation, and surface deposition of suspended sediments and organic litter. The model relies heavily on the characteristics derived from soil cores, including bulk density, percent organic matter, and rates of mass accumulation obtained from radioisotope dating or surface elevation

tables (SETs). Multiple competing plant species can be simulated at once to understand how habitat may evolve for species of concern. WARMER3 builds upon WARMER2 (another 1D soil cohort model) in multiple ways. WARMER2 uses a more direct calibration of observed organic accumulation rates, while WARMER3 uses estimates of productivity, root turnover, and decomposition to generate organic soil material. Both models rely on calibration with soil cores, WARMER3 explicitly models belowground processes in more detail, allowing for finer calibration to observational datasets, such as the proportion of dead to living roots, root size-specific turnover rates, and treatment of aboveground litter material.

Soil core mineral and organic matter accumulation rates were calculated for each soil core based on the depth profiles of bulk density and percent organic matter and the accretion rate determined from either  $^{210}\text{Pb}$  or  $^{137}\text{Cs}$  dating. An effective suspended sediment concentration (SSC) for each site was determined through model calibration and a 50-year hindcast; we

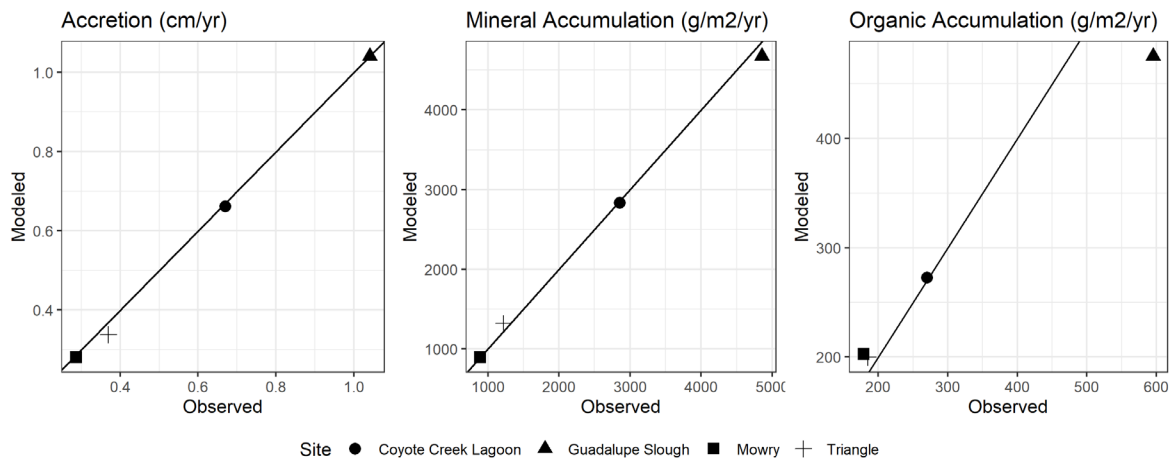


**Figure 3.** Comparison of modeled and observed accretion and mass accumulation rates from the 50-year hindcast. Solid line is 1:1.

leveraged the observed accretion rate, historic sea-level rise rate, and surface elevation of the soil core to calculate the relative elevation of the soil surface 50 years in the past. A 100-year spin-up period is used to establish initial vegetation cover and soil characteristics and then the model was run forward. Depth profiles of bulk density were used to constrain the minimum and maximum soil porosity. Calibration of the compaction rate and the decomposition rate was completed using an optimization scheme to minimize the differences among modeled and observed accretion rate and mass accumulation rates (Fig. 3). Model parameters for each site and species are provided in tables 1 and 2.

There is relatively little information available on root size and depth distributions, turnover rates, or composition for the common marsh species found in San Francisco Bay. As such, where no information was available, we kept parameter values the same across species and relied on calibration of soil characteristics depth profiles. Prior sensitivity analysis has found WARMER3 to be relatively insensitive to these parameter choices (Buffington et al. 2024). At Mowry, Triangle, and Guadalupe Slough sites we assumed *Salicornia pacifica* and *Spartina foliosa* were the dominant marsh species at high and low marsh elevations, respectively, while at the more brackish Coyote Creek Lagoon site we assumed the marsh would continue to be dominated by *Schoenoplectus americanus*. These assumptions were made based on the dominant species observed during vegetation surveys at each site (Rankin et al. 2024).

### **Model scenarios**

Future vulnerability of each marsh to SLR was assessed by simulating range of SLR scenarios from the interagency SLR report (Sweet et al 2022, access via <https://sealevel.nasa.gov/task-force->

scenario-tool). We selected four projections for our analysis, low, intermediate, intermediate high, and high (Fig. 4), which are based on greenhouse gas emission trajectories. These scenarios were selected because they cover the range of potential societal responses and uncertainty regarding ice sheet dynamics. In addition to SLR, we also explored the sensitivity of model projections to a range of sediment availability scenarios, changing SSC  $\pm$  50%. Key model inputs of initial elevation and maximum biomass were randomly altered using a Monte Carlo simulation framework, with parameter values selected from a normal distribution. Initial elevation was sampled from a distribution with a standard deviation of 2 cm, which is the stated accuracy of survey-grade elevation measurements. A standard deviation of 10% was selected for maximum biomass to propagate uncertainty related to organic accumulation. Similarly, we used a 10% standard deviation in suspended sediment concentration. Finally, we incorporated interannual variation in mean sea level into the projections by randomly sampling from a Weibull distribution that was derived from the residuals of a linear regression of mean sea level at the Golden Gate NOAA gauge (1972-2022; station: 9414290). WARMER3 was run 1000 times under each scenario at initial elevations that stretched across the range of the bias-corrected DEM (Buffington and Thorne 2019) and in 5 cm intervals. Mean and standard deviation of modeled elevation, wetland area, carbon accumulation, and species cover were calculated and then interpolated across a DEM clipped to the current extent of each marsh. We assumed there was no upslope migration space available at these sites since they are bounded on their upper edge by levees or roads.

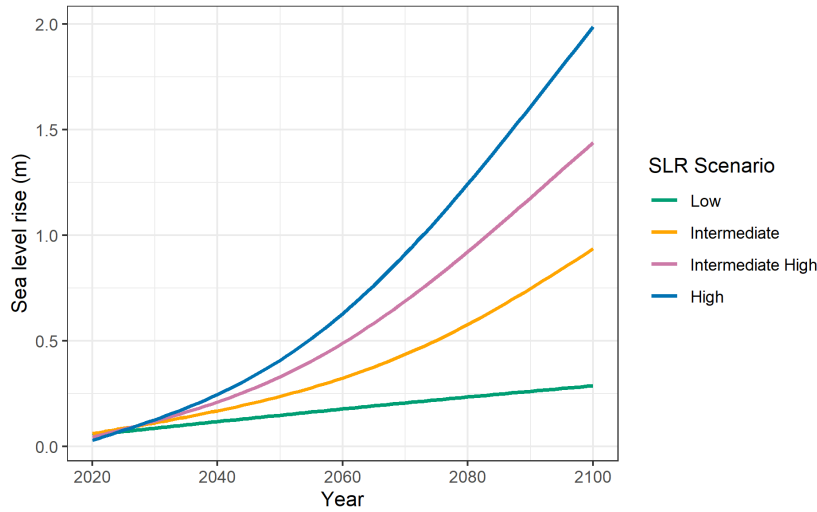


**Figure 4.** Selected sea-level rise scenarios from the NOAA interagency report (Sweet et al. 2022).

**Table 1.** WARMER3 site-level parameters.

Parameter	Mowry	Triangle	Guadalupe	Coyote	units	Source
			Slough	Creek	Lagoon	
Effective suspended sediment concentration	100	90	520	250	mg L <sup>-1</sup>	Calibration
Tide range	2.59	2.69	2.96	2.69	m	NOAA gauge
Decomposition rate	0.0006	0.0005	0.0004	0.0006	d <sup>-1</sup>	Calibration
Decomposition flood sensitivity	1.1	1.1	1.1	1.1	-	Calibration
Surface organic deposition fraction	0.05	0.05	0.1	0.05	-	Calibration
Minimum porosity	0.6	0.6	0.5	0.6	-	Calibration
Maximum porosity	0.88	0.88	0.88	0.88	-	Constant
Maximum porosity change	0.05	0.05	0.05	0.05	y <sup>-1</sup>	Constant
Compaction rate	1.7	2.5	1.8	2.0	cm <sup>3</sup> g <sup>-1</sup>	Calibration
Initial soil organic fraction	0.1	0.1	0.1	0.1	-	Soil cores
Organic matter density	0.5	0.5	0.5	0.5	g cm <sup>3</sup>	Constant

**Table 2.** WARMER3 plant species parameters.

Parameter	<i>Spartina</i>	<i>Salicornia</i>	<i>Schoenoplectus</i>	units	Source
	<i>foliosa</i>	<i>pacifica</i>	<i>americanus</i>		
Maximum biomass	2000	3000	1600	g m <sup>-2</sup>	Kirwan and
Structural root fraction	0.4	0.4	0.76	-	Guntenspergen 2012
Fine root fraction	0.7	0.7	0.8	-	Janousek et al. 2016;
Root:Shoot	function	function	1.8	-	Calibration
Rooting depth	0.4	0.4	0.6	m	Estimated
Fine root turnover	0.5	0.4	0.75	y <sup>-1</sup>	Calibration
Coarse root turnover	0.15	0.15	0.4	y <sup>-1</sup>	Calibration
Structural root turnover	0.05	0.05	0.1	y <sup>-1</sup>	Calibration
Fine root particulate rate	0.5	0.5	0.2	y <sup>-1</sup>	Calibration
Fine root labile fraction	0.3	0.3	0.3	-	Constant
Large root labile fraction	0.5	0.5	0.5	-	Constant
Litter deposition rate	0.25	0.25	0.4	y <sup>-1</sup>	Calibration
Leaf litter fraction	1.0	0.75	1.0	-	
Leaf refractory fraction	0.5	0.5	0.5	-	Constant
Litter deposition fraction	0.1	0.1	0.4	-	Calibration
Growth rate	0.3	0.3	0.2	y <sup>-1</sup>	
Wood density	NA	0.4	NA	g cm <sup>-3</sup>	
Root density	0.1	0.1	0.1	g cm <sup>-3</sup>	Bouma et al. 2003

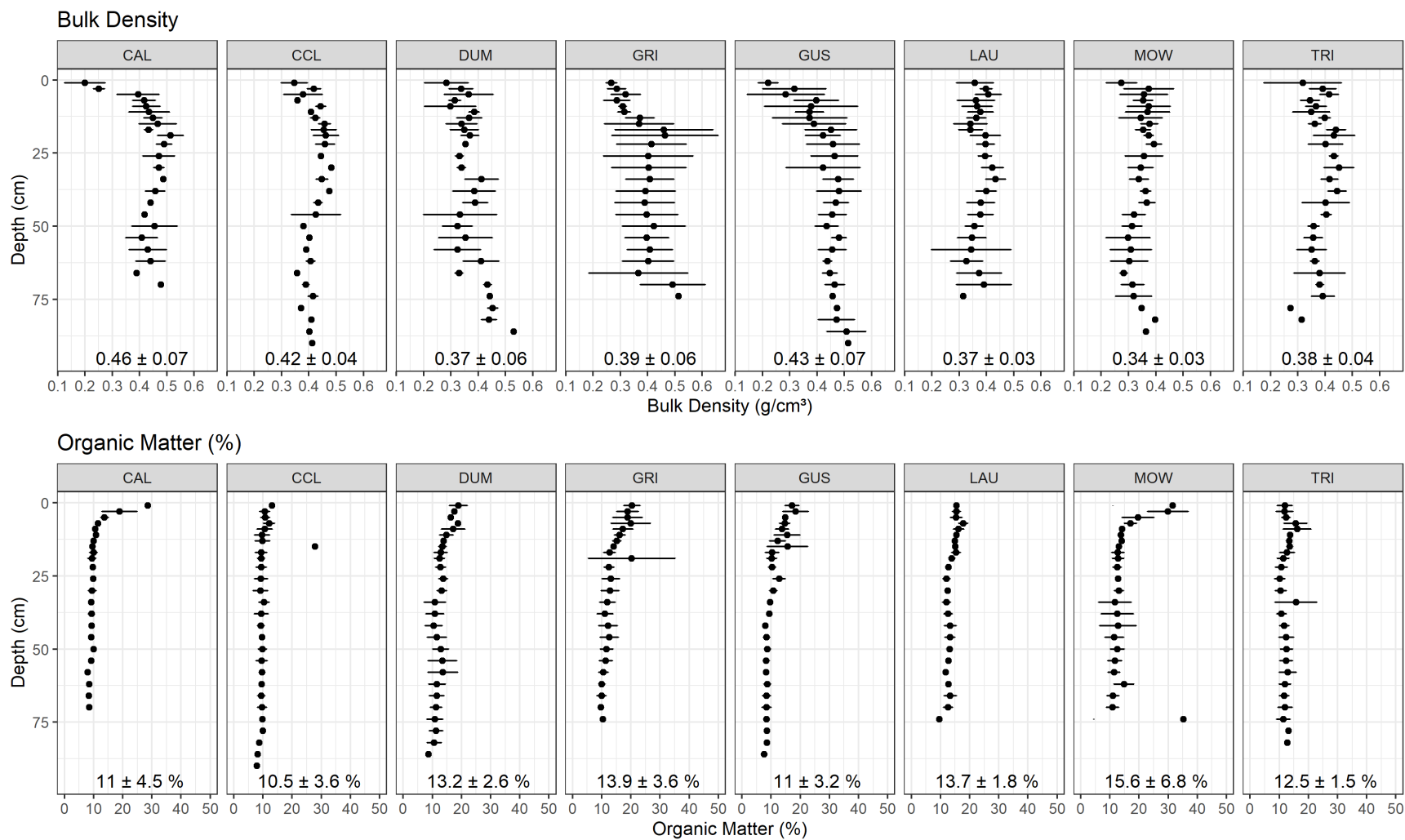


**Figure 5.** Soil core properties (mean  $\pm$  SD) across eight tidal marsh parcels in south San Francisco Bay. [CAL=Calaveras; CCL=Coyote Creek Lagoon; DUM=Dumbarton; GRI=Greco Island; GUS=Guadalupe Slough; LAU=Laumeister; MOW=Mowry; TRI=Triangle]

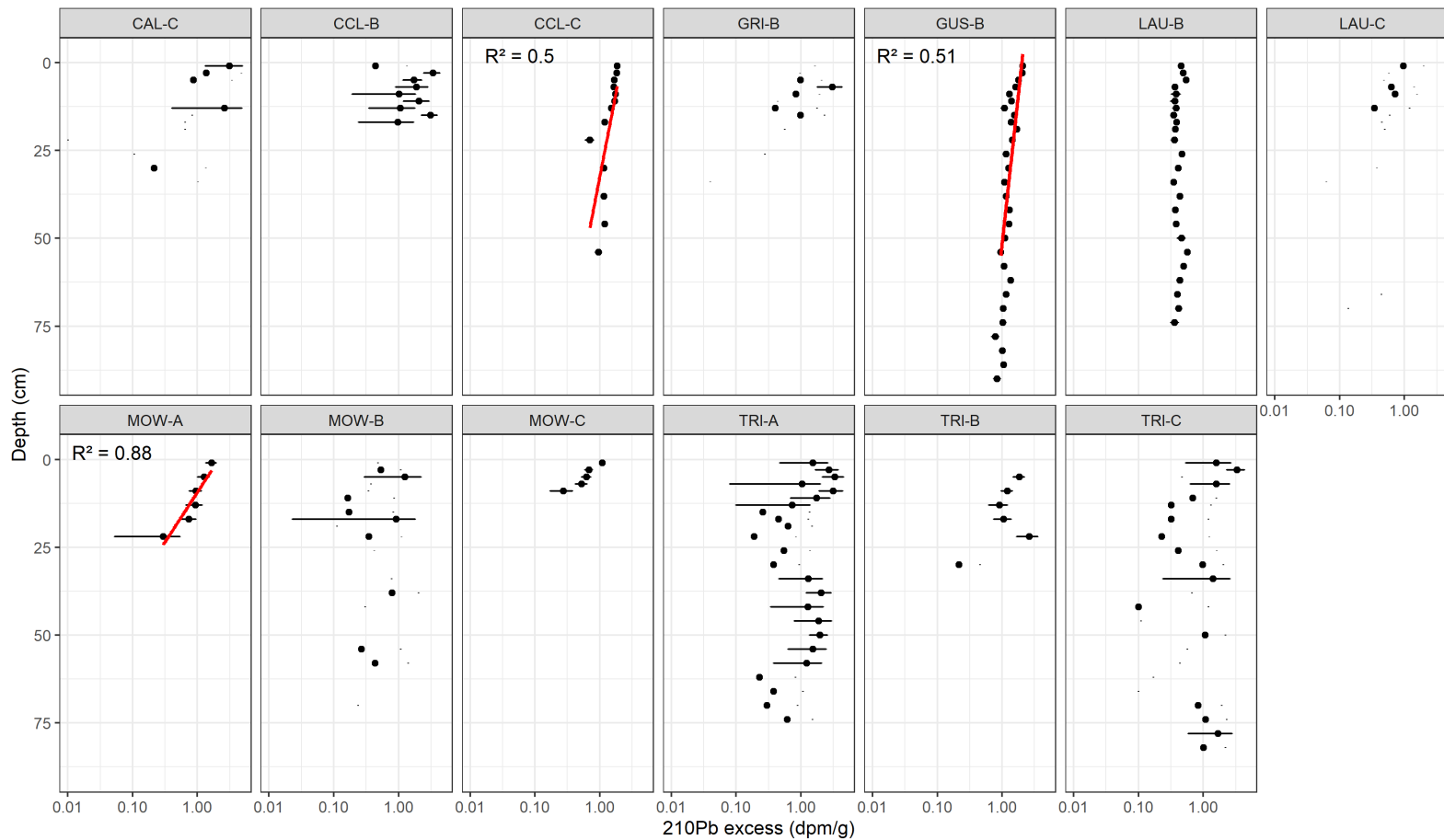


**Figure 6.** Down-core excess  $^{210}\text{Pb}$  activity (disintegrations per minute/gram). Cores with the regression line met the assumptions needed for calculating ages of each interval. [CAL=Calaveras; CCL=Coyote Creek Lagoon; DUM=Dumbarton; GRI=Greco Island; GUS=Guadalupe Slough; LAU=Laumeister; MOW=Mowry; TRI=Triangle]

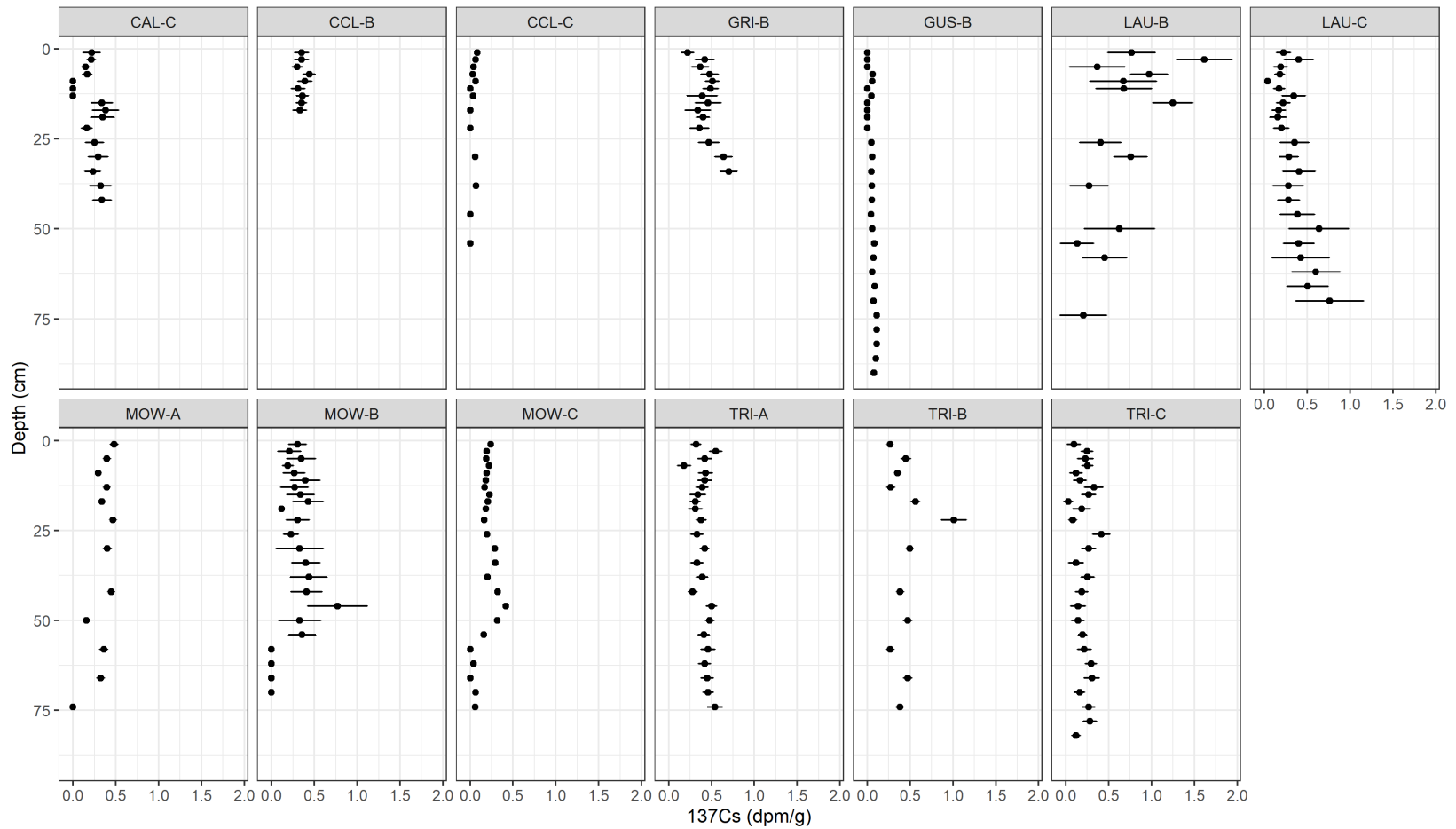


**Figure 7.** Down-core  $^{137}\text{Cs}$  activities (disintegrations per minute/gram). TRI-B was the only core with a distinct peak in Cs activity.

[CAL=Calaveras; CCL=Coyote Creek Lagoon; DUM=Dumbarton; GRI=Greco Island; GUS=Guadalupe Slough; LAU=Laumeister;

MOW=Mowry; TRI=Triangle]

## Results

### *Soil characteristics*

Downcore bulk densities averaged  $0.39 \pm 0.05 \text{ g cm}^{-3}$  (n=22) and percent organic matter averaged  $12.7 \pm 3.8\%$  (n=20; Fig. 5). Site-level differences in bulk density were not significant ( $F_{7,14}=1.36$ ,  $p=0.295$ ). Differences in percent organic matter were significant ( $F_{7,12}=3.594$ ,  $p=0.025$ ), however exploration of pair-wise differences with the Tukey HSD test revealed no significance at the  $\alpha=0.05$  level. Using an established relationship between percent organic matter and percent carbon ( $\%C = 0.001217*\%OM^2 + 0.3839*\%OM$ ; Callaway et al., 2012), we found carbon stocks down to 50 cm of  $93.0 \pm 14.2 \text{ Mg SOC ha}^{-1}$  (n=20). Differences in SOC across sites were not significantly different ( $F_{7,12}=0.64$ ,  $p=0.71$ ).

### *Accretion rates*

Three soil cores had excess  $^{210}\text{Pb}$  depth profiles that could be used for calculating accretion rates and one had a peak in  $^{137}\text{Cs}$  (Figs. 6 & 7, Table 3). Both Mowry and Triangle had accretion rates near the long-term historic SLR rate of  $0.2 \text{ cm yr}^{-1}$ , while both Coyote Creek Lagoon and Guadalupe Slough had accretion rates greater than the long-term SLR rate.

**Table 3.** Summary of accretion and mass accumulation rates (mean, standard deviation) from successfully dated soil cores. The rates from the  $^{210}\text{Pb}$  dated cores are from ~1972-2022, while the rate from  $^{137}\text{Cs}$  assumed that peak activity occurred in 1963.

Site	Core ID	Dating method	Accretion (cm yr <sup>-1</sup> )	Mineral accumulation (g m <sup>-2</sup> yr <sup>-1</sup> )	Organic accumulation (g m <sup>-2</sup> yr <sup>-1</sup> )
Coyote Creek Lagoon	CCL-C	<sup>210</sup> Pb	0.67 (0.32)	2856.0 (1185.0)	270.2 (102.6)
Guadalupe Slough	GUS-B	<sup>210</sup> Pb	0.91 (0.35)	4585.7 (1624.7)	595.6 (249.3)
Mowry	MOW-A	<sup>210</sup> Pb	0.29 (0.09)	889.0 (293.3)	179.0 (81.8)
Triangle	TRI-B	<sup>137</sup> Cs	0.38	1220.4	185.0

*WARMER3 projections*

*Relative elevation and plant cover with SLR*

Under low SLR, marsh elevation was projected to increase slightly across all sites (Fig. 8) and species composition was projected to remain relatively consistent (Fig. 9) illustrating resilience. In the intermediate SLR scenario, Guadalupe Slough elevation increased until ~2060 and then declined to roughly the starting relative elevation and species cover remained consistent, while at Mowry and Triangle a transition to *Spartina* was projected for the second half of the century. With the intermediate high and high scenarios, all sites were projected to decline in relative elevation, transition to *Spartina*, and in the cases of Mowry and Triangle, convert to an unvegetated state (Figs 9, 10). The transition to an unvegetated state was projected at Coyote

Creek Lagoon only under the high SLR scenario, while Guadalupe Slough was projected to remain a vegetated marsh until 2100 under all SLR scenarios.

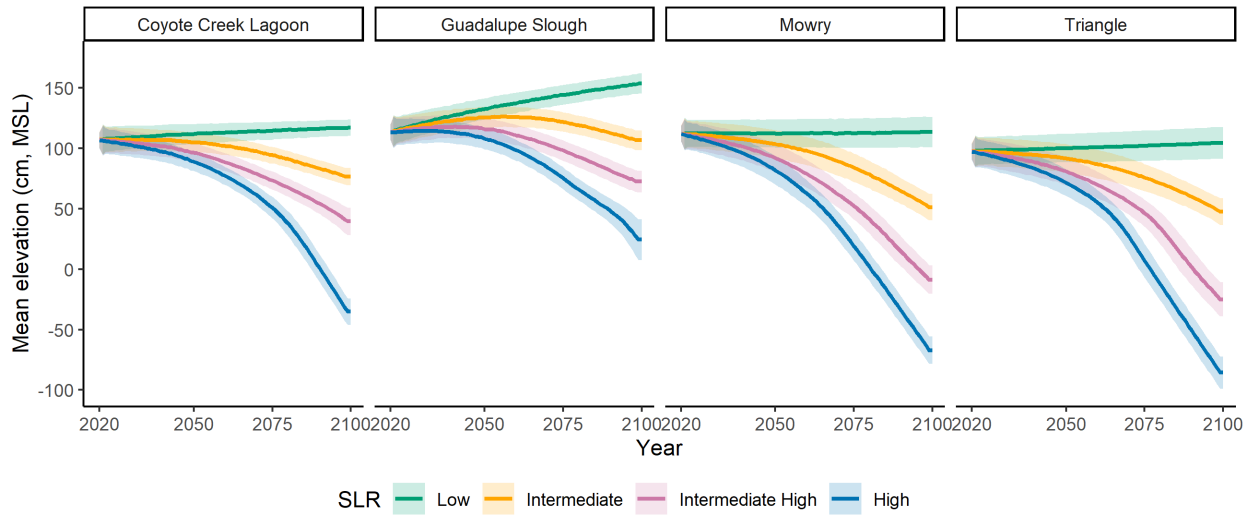


**Figure 8.** Mean marsh elevation across sea-level rise scenarios. Shading represents the standard deviation from Monte Carlo simulations.

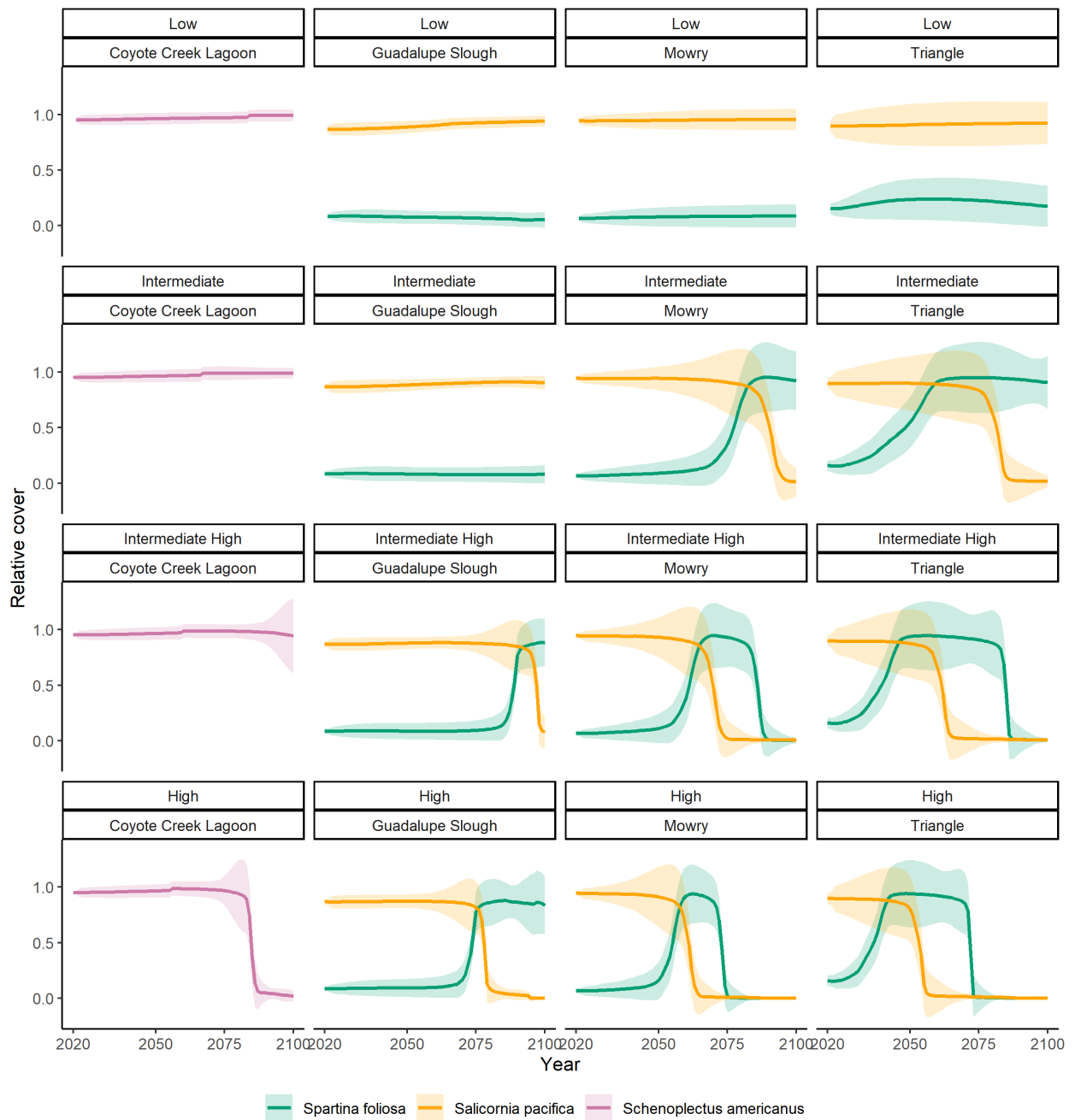


**Figure 9.** Mean cover of the dominant marsh species by marsh across sea-level rise scenarios.

Shading represents the standard deviation from Monte Carlo simulations.

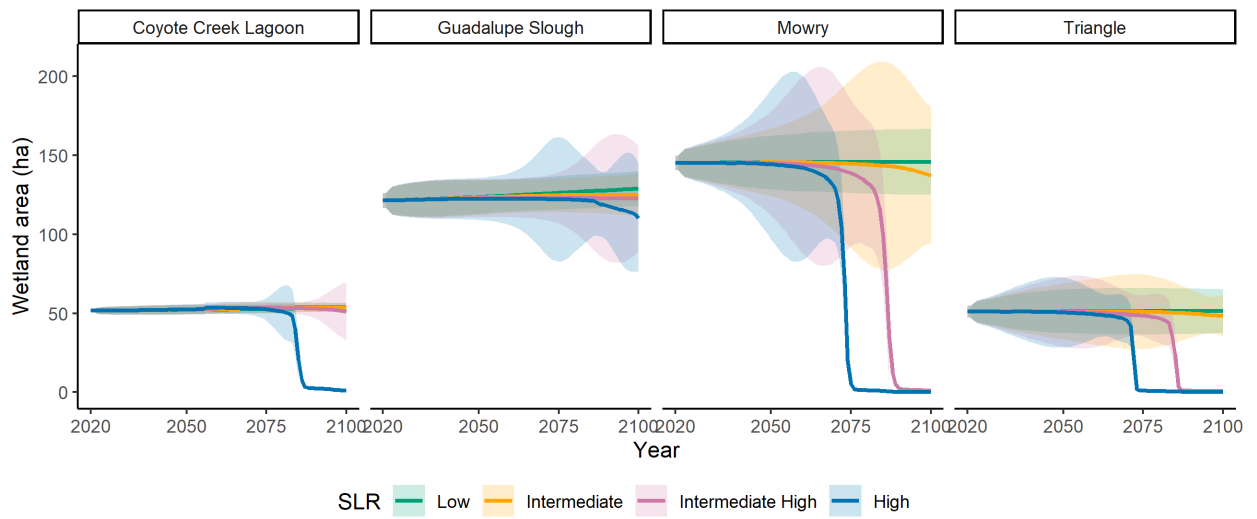


**Figure 10.** Vegetated wetland area (ha) across sea-level rise scenarios. Shading represents the standard deviation from Monte Carlo simulations.

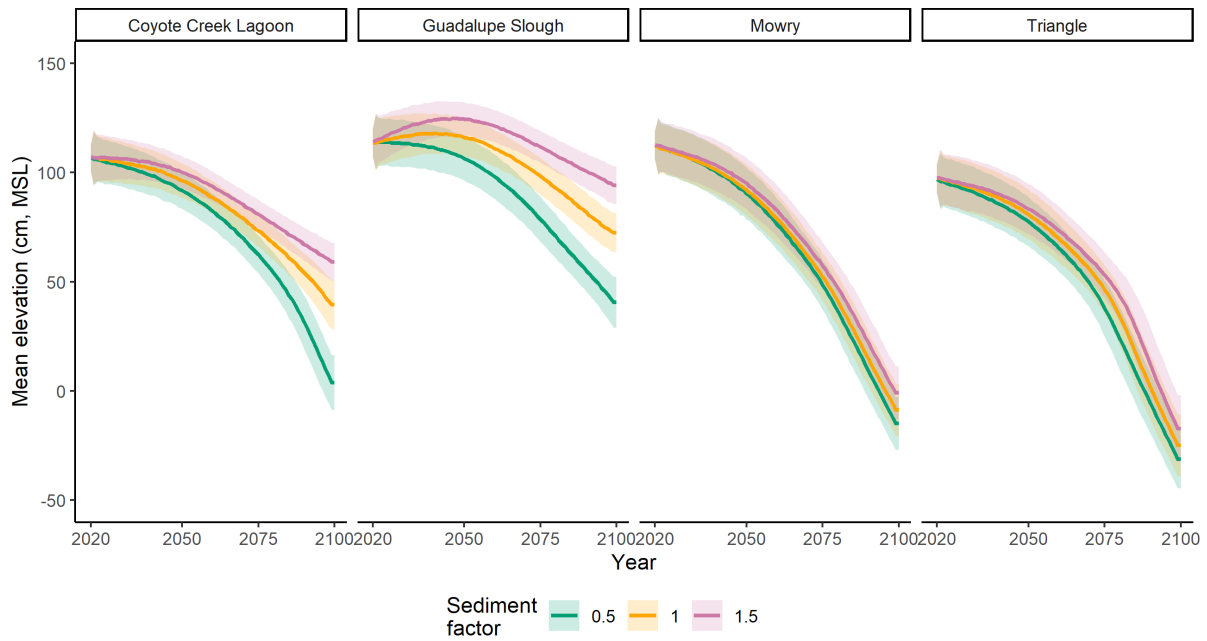


**Figure 11.** Mean elevation (cm, relative to mean sea level) projected under the intermediate high scenario across a range of sediment scenarios (0.5=50% suspended sediment concentration, 1=100% suspended sediment concentration, 1.5=150% suspended sediment concentration).

#### *Sediment scenarios*

Altering the calibrated suspended sediment by -50% or +50% resulted in relatively minor changes in the elevation trajectory at Mowry and Triangle, while at Coyote Creek Lagoon and Guadalupe Slough, sites with higher calibrated SSC, the changes in elevation were more dramatic (Fig. 11). A 50% decline in SSC at Coyote Creek Lagoon and Guadalupe Slough lead to the loss of vegetated marsh and transition to *Spartina foliosa*, respectively. A 50% increase in SSC slowed the rate of relative elevation loss at both sites and plant cover was maintained.

#### *Carbon storage*

Carbon accumulation rates were projected to change with site- and sea-level rise scenario-specific differences (Fig. 12). At Guadalupe Slough, carbon accumulation was projected to decline slightly until mid-century, then increase or stabilize under the intermediate, intermediate high, and high SLR scenarios. At Mowry and Triangle, the timing of projected declines in carbon accumulation corresponded to the changes in dominant plant cover. Carbon accumulation was projected to first increase at Coyote Creek Lagoon under the three highest SLR scenarios, with declines projected in the highest two SLR scenarios commensurate with declines in plant cover.

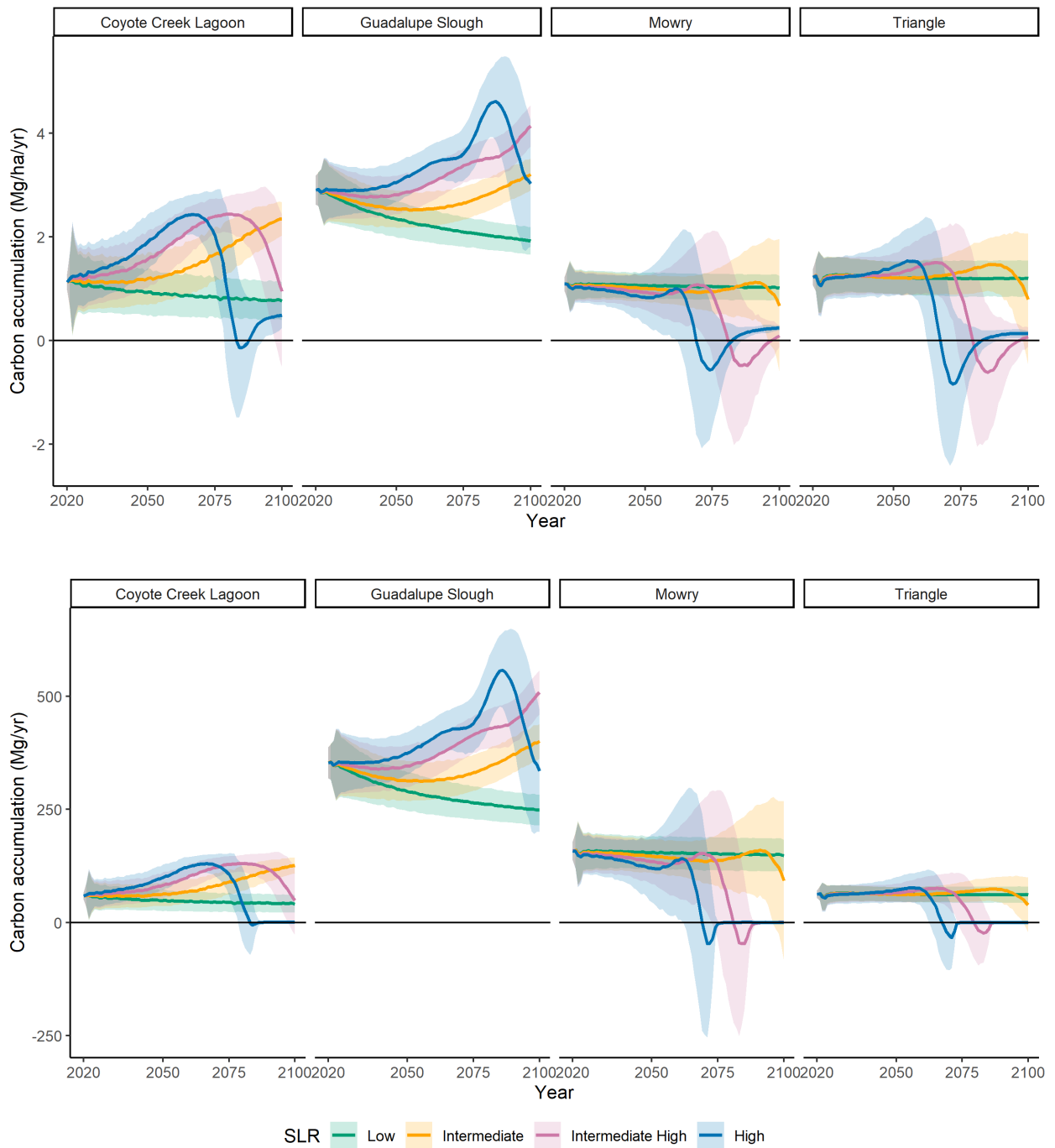


**Figure 12.** Mean carbon accumulation rate ( $\text{Mg ha}^{-1} \text{yr}^{-1}$ ) across sea-level rise scenarios (top) and total carbon accumulation across each site ( $\text{Mg yr}^{-1}$ ). Shading represents the standard deviation from Monte Carlo simulations.

## Discussion

### *Alternative marsh futures*

The fate of tidal marshes in south San Francisco Bay depends heavily on the realized rates of SLR. Under low or intermediate scenarios, the natural processes that marshes rely on to build elevation are likely to be able to keep up with SLR. Under the higher scenarios of 1.5 to 2 m of SLR by 2100, however, extensive changes to the structure and function of the tidal marshes appears likely as three of the four marshes we examined were projected to become unvegetated. Increases in suspended sediment availability were shown to increase marsh resilience, in some cases delaying or preventing the transition to an unvegetated state. Under intermediate high and high SLR projections, the model suggests that wildlife species that rely on the *Salicornia* marsh that currently dominates DENWR may be at further risk of population declines with SLR as marsh vegetation transitions to *Spartina*. Alternatively, species that prefer *Spartina* may benefit, at least temporarily, from the transition of habitat to the more flooding tolerant plant species.

### *Determining accretion rates*

We had difficulty dating soil cores, with just four of 13 cores providing reliable accretion rates from radioisotopes. We suspect that the sediments in south San Francisco Bay are subject to extensive redistribution from the expansive mudflats, which makes the radioisotope method for estimating accretion rates unreliable. The Constant Rate of Supply (CRS) model assumes  $^{210}\text{Pb}$  is

constantly being deposited on the marsh surface, either directly from the atmosphere (rainfall) or attached to sediments from the watershed that are deposited onto the marsh surface. The process is likely different across DENWR marshes. Sediment is mixed from various watersheds across the mudflat and subsequent redistribution by tides and wind-waves (Schoellhamer 1996) results in a delay in marsh deposition that may invalidate the CRS model assumptions. Additionally, some areas around the bay are experiencing edge erosion (WinklerPrins et al. 2024), a process that will also redistribute sediment and introduce further variation in the radioactivity of deposited sediments. Finally, regular precipitation is needed for  $^{210}\text{Pb}$  deposition and the Mediterranean climate of San Francisco Bay may simply not generate enough  $^{210}\text{Pb}$  for *in situ* deposition. All together these factors contribute to a downcore radioactivity profile that is too mixed to be reliable for calculating accretion rates.

From the soil cores we were able to successfully date, we found that DENWR marshes are keeping pace with the current rate of SLR. The relatively high accretion rate at Guadalupe Slough and Coyote Creek Lagoon suggests that additional processes may be occurring that are causing a decrease in marsh elevation, such as deep subsidence from fluid extraction or soil consolidation. Additionally, both marshes are located close to fluvial sediment sources that may deposit sediment in large amounts during high flow events. Established marshes that are high in the tide frame would show relatively high accretion rates in soil cores if they were experiencing subsidence, provided there is sufficient sediment available for deposition to fill in the accommodation space that is created (Rogers et al. 2022), while marshes lower in the tide frame can experience rapid accretion without subsidence since they experience more regular tidal flooding. Subsidence rates are difficult to measure in marshes and can vary widely across small

spatial areas, thus we did not explicitly account for it in the WARMER3 projections. A dedicated effort to measure deep subsidence around San Francisco Bay marsh, for example, through repeated measurements of surface elevation tables (SETs), would provide valuable data that could be included in future modeling efforts. Shorter-term deposition studies can also be used to help determine the contribution of storms and fluvial discharge to marsh sediment budgets.

Measurements of deposition and elevation change via marker horizons and SETs provide more robust measures of marsh deposition and elevation change. About one year of SET data at Mowry (K. Thorne, U.S. Geological Survey, unpublished data, 2024) showed high rates of accretion ( $0.5 \text{ cm yr}^{-1}$ ) and net elevation change ( $0.68 \text{ cm yr}^{-1}$ ), higher than historic rate of  $0.29 \text{ cm yr}^{-1}$  from the  $^{210}\text{Pb}$  dating. While the current record of measurement at the SETs (installed in 2022) is too short to be useful for calibration of a long-term projection model like WARMER3, the accretion data from them will be extremely valuable in future years as a tool for monitoring marsh elevation dynamics with SLR.

There is a lack of knowledge of the belowground characteristics of most Pacific coast tidal marsh plants. Knowledge gaps exist on root size distributions, turnover rates, and tissue composition (e.g., percent lignin). Dedicated study to understanding these characteristics across flooding and nutrient gradients would greatly benefit our ability to simulate tidal marsh responses to environmental changes.

## References

- Blum, L.K., 1993. *Spartina alterniflora* root dynamics in a Virginia marsh. *Marine Ecology Progress Series*, 102, pp.169-178.
- Boorman, L.A., Garbutt, A. and Barratt, D., 1998. The role of vegetation in determining patterns of the accretion of salt marsh sediment. *Geological Society, London, Special Publications*, 139(1), pp.389-399.
- Buffington, K.J., Janousek, C.N., Dugger, B.D., Callaway, J.C., Schile-Beers, L.M., Borgnis Sloane, E. and Thorne, K.M., 2021. Incorporation of uncertainty to improve projections of tidal wetland elevation and carbon accumulation with sea-level rise. *Plos one*, 16(10), p.e0256707.
- Buffington, K.J., Carr, J.A., MacKenzie, R.A., Apwong, M., Krauss, K.W. and Thorne, K.M., 2024. Projecting mangrove forest resilience to sea-level rise on a Pacific Island: species dynamics and ecological thresholds. *Estuaries and Coasts*, 47(8), pp.2174-2189.
- Buffington, K.J., and Thorne, K.M., 2019, LEAN-corrected San Francisco Bay digital elevation model, 2018: U.S. Geological Survey data release, <https://doi.org/10.5066/P97J9GU8>.
- Cahoon, D.R., 2015. Estimating relative sea-level rise and submergence potential at a coastal wetland. *Estuaries and Coasts*, 38(3), pp.1077-1084.
- Callaway, J. C., Borgnis, E. L., Turner, R. E., & Milan, C. S. (2012). Carbon Sequestration and Sediment Accretion in San Francisco Bay Tidal Wetlands. *Estuaries and Coasts*, 35(5), 1163–1181. <https://doi.org/10.1007/s12237-012-9508-9>

- Don Edwards San Francisco Bay National Wildlife Refuge: final comprehensive conservation plan. (2012). Don Edwards San Francisco Bay National Wildlife Refuge, U.S. Fish and Wildlife Services. <https://purl.fdlp.gov/GPO/gpo51796>
- Gosselink, J.G., Hatton, R. and Hopkinson, C.S., 1984. Relationship of organic carbon and mineral content to bulk density in Louisiana marsh soils. *Soil Science*, 137(3), pp.177-180.
- Howarth, R.W. and Hobbie, J.E., 1982. The regulation of decomposition and heterotrophic microbial activity in salt marsh soils: a review. *Estuarine comparisons*, pp.183-207.
- Janousek, C.N., Buffington, K.J., Thorne, K.M., Guntenspergen, G.R., Takekawa, J.Y. and Dugger, B.D., 2016. Potential effects of sea-level rise on plant productivity: species-specific responses in northeast Pacific tidal marshes. *Marine Ecology Progress Series*, 548, pp.111-125.
- Kirwan, M.L. and Guntenspergen, G.R., 2012. Feedbacks between inundation, root production, and shoot growth in a rapidly submerging brackish marsh. *Journal of Ecology*, 100(3), pp.764-770.
- Kirwan, M.L. and Megonigal, J.P., 2013. Tidal wetland stability in the face of human impacts and sea-level rise. *Nature*, 504(7478), pp.53-60.
- MacKenzie, R.A., Foulk, P.B., Klump, J.V., Weckerly, K., Purbospito, J., Murdiyarso, D., Donato, D.C. and Nam, V.N., 2016. Sedimentation and belowground carbon accumulation rates in mangrove forests that differ in diversity and land use: a tale of two mangroves. *Wetlands Ecology and Management*, 24, pp.245-261.

- Morris, J.T., Drexler, J.Z., Vaughn, L.J. and Robinson, A.H., 2022. An assessment of future tidal marsh resilience in the San Francisco Estuary through modeling and quantifiable metrics of sustainability. *Frontiers in Environmental Science*, 10, p.1039143.
- Rankin, L.L., Jones, S.F., Janousek, C.N., Buffington, K.J, Takekawa, J.Y., and Thorne, K.M., 2024, Marsh vegetation surveys across the San Francisco Bay Estuary, 2008-2018: U.S. Geological Survey data release, <https://doi.org/10.5066/P94F802H>.
- Ritchie, J.C. and McHenry, J.R., 1990. Application of radioactive fallout cesium-137 for measuring soil erosion and sediment accumulation rates and patterns: A review. *Journal of environmental quality*, 19(2), pp.215-233.
- Rogers, K., Zawadzki, A., Mogensen, L.A. and Saintilan, N., 2022. Coastal wetland surface elevation change is dynamically related to accommodation space and influenced by sedimentation and sea-level rise over decadal timescales. *Frontiers in Marine Science*, 9, p.807588.
- Schile, L.M., Callaway, J.C., Morris, J.T., Stralberg, D., Parker, V.T. and Kelly, M., 2014. Modeling tidal marsh distribution with sea-level rise: evaluating the role of vegetation, sediment, and upland habitat in marsh resiliency. *PloS one*, 9(2), p.e88760.
- Schoellhamer, D.H., 1996. Factors affecting suspended-solids concentrations in south San Francisco Bay, California. *Journal of Geophysical Research: Oceans*, 101(C5), pp.12087-12095.

- Stagg, C.L., Schoolmaster, D.R., Krauss, K.W., Cormier, N. and Conner, W.H., 2017. Causal mechanisms of soil organic matter decomposition: deconstructing salinity and flooding impacts in coastal wetlands. *Ecology*, 98(8), pp.2003-2018.
- Stumpf, R.P., 1983. The process of sedimentation on the surface of a salt marsh. *Estuarine, Coastal and Shelf Science*, 17(5), pp.495-508.
- Swanson, K.M., Drexler, J.Z., Schoellhamer, D.H., Thorne, K.M., Casazza, M.L., Overton, C.T., Callaway, J.C. and Takekawa, J.Y., 2014. Wetland accretion rate model of ecosystem resilience (WARMER) and its application to habitat sustainability for endangered species in the San Francisco estuary. *Estuaries and Coasts*, 37, pp.476-492.
- Sweet, W.V., Hamlington, B.D., Kopp, R.E., Weaver, C.P., Barnard, P.L., Bekaert, D., Brooks, W., Craghan, M., Dusek, G., Frederikse, T. and Garner, G., 2022. Global and Regional Sea Level Rise Scenarios for the United States: Updated Mean Projections and Extreme Weather Level Probabilities along US Coastlines.
- Thorne, K. M., Backe, K. E., Freeman, C. M., Buffington, K. J., Forstner, T. M., and Goodman, A. C. 2019. Don Edwards National Wildlife Refuge Vegetation, Elevation, Inundation Inventory to Inform Sea-level Rise Vulnerability. Unpubl. Data Summary Report. USGS Western Ecological Research Center, Davis, CA. 112pp.
- Thorne, K.M., Buffington, K.J., Osland, M.J., Chivoiu, B., Grace, J.B., Enwright, N.M. and Guntenspergen, G.R., 2025. Nature-based solutions could offset coastal squeeze of tidal wetlands from sea-level rise on the US Pacific coast. *Scientific reports*, 15(1), p.11443.

WinklerPrins, L., Lacy, J.R., Stacey, M.T., Logan, J.B. and Stevens, A.W., 2024. Seasonality of retreat rate of a wave-exposed marsh edge. *Journal of Geophysical Research: Earth Surface*, 129(7), p.e2023JF007468.

Wright, L.D. and Thom, B.G., 2023. Coastal morphodynamics and climate change: A review of recent advances. *Journal of Marine Science and Engineering*, 11(10), p.1997.